Resolvent-Based ROM and Feedback Control for NACA0012 Airfoil Flow

Pengxiao Jiang [1, *], Bo jin [1]

[1] Nanjing University of Aeronautics and Astronautics, China.

Abstract. This study investigates resolvent-based model reduction and robust feedback control for separated flow over a NACA0012 airfoil at low Reynolds number. The incompressible Navier–Stokes equations are linearized about a steady base flow, and the resulting resolvent operator is sampled in the frequency domain. A low-order input–output model is then identified via vector fitting, yielding a reduced-order model that accurately reproduces the frequency response and impulse dynamics of the full system. Based on this model, an H-infinity loop-shaping controller is designed and tuned through appropriate weighting functions. The closed-loop simulations demonstrate global suppression of separation and a significant reduction of perturbation energy. Further, a sensor-placement study is conducted through a spatial traversal optimization. The results reveal a strong correlation between the optimal stability margin and the pole–zero separation, highlighting how non-minimum-phase behavior fundamentally limits achievable robustness and providing a physically interpretable guideline for sensor placement in airfoil flow control.

Keywords: Flow control; Resolvent operator; Reduced-order model; H_∞control.

1. Introduction

Flow separation and unsteady vortex shedding in airfoil flows are classical fluid mechanics problems. At low Reynolds numbers, these phenomena significantly degrade aerodynamic performance, causing lift reduction, drag increase, and structural vibration. Over the past decades, researchers have developed various flow control strategies, including passive geometric modifications and active open-loop methods like blowing/suction and synthetic jets applied to the boundary layer [1, 2]. However, these methods lack real-time sensing and response capabilities, making them less adaptable to dynamic operating conditions. Active open-loop control, relying on preset frequencies, often lacks robustness against free stream changes or external disturbances.

Feedback control offers superior performance and robustness by dynamically adjusting actuation based on real-time sensor data. However, applying it to fluid systems governed by the Navier-Stokes equations is challenging due to their high dimensionality (millions of state variables) and strong nonlinearity. This prohibitive computational cost prevents the direct application of modern control algorithms. Therefore, developing Reduced-Order Models (ROMs) that accurately capture key flow dynamics is essential for enabling fluid feedback control.

In reduced-order modeling, beyond traditional POD methods, input-output analysis based on the Resolvent Operator of linearized Navier-Stokes equations has gained significant attention. McKeon and Sharma framed nonlinear terms as internal forcing [3], and Towne et al. linked resolvent modes to energetic coherent structures (SPOD modes) [4]. Sipp and Marquet highlighted its advantage in modeling unstable systems without frequency limitations [5]. Furthermore, Symon et al, Yeh and Taira successfully applied this method to analyze energy amplification in cylinder flows and optimize open-loop control for airfoil separation [6, 7], validating its effectiveness for complex flows.

This paper addresses flow separation and unsteady vortex shedding on a NACA0012 airfoil at low Reynolds numbers. We adopt an efficient modeling and control framework (Jin et al. [8]) centered on system identification using the resolvent operator. This method captures input-output dynamics directly from frequency responses, avoiding time-consuming transient simulations. We identify an accurate ROM using vector fitting and design a robust feedback controller using Glover & McFarlane's H-infinity loop-shaping method [9]. The controller's effectiveness is validated via high-fidelity Direct Numerical Simulation (DNS).

2. Method

2.1 Linearized Modeling and Model Reduction Methods

To design effective feedback control for the flow field, it is first necessary to establish a linear state-space model that can accurately describe the fluid dynamic characteristics. Referring to Jin's derivation framework, linearizes the incompressible Navier-Stokes equations near the steady base flow (U,P) and describes them in generalized eigenvalue form:

$$sEx = Ax + \hat{f} \tag{1}$$

Where A is the Navier-Stokes operator based on the linearization of the basis current, and E is the mass matrix, which is defined in the following form:

$$A = \begin{bmatrix} -U\cdot\nabla - (\,)\cdot\nabla U + \nu\nabla^2 & -\nabla \\ \nabla\cdot(\,) & 0 \end{bmatrix} \quad E = \begin{bmatrix} I & 0 \\ 0 & 0 \end{bmatrix} \tag{2}$$

The flow field system can be represented in the form of a standard linear time-invariant (LTI) system:

$$\begin{aligned} sEx &= Ax + Be \\ y &= Cx + De \end{aligned} \tag{3}$$

Matrix B determines the spatial distribution and shape of the actuator, C determines the position of the sensor, and D is the direct transfer matrix, which is usually 0 in fluid systems. Therefore, the transfer function G(s) from the control input e to the measured output y can be expressed as:

$$G(s) = C(sE - A)^{-1}B + D \tag{4}$$

The spatially discretized system state has an extremely high dimensionality (N~10^5). Therefore, we use system identification methods to construct a reduced-order model:

$$\tilde{G}(s) = \sum_{m=1}^{N_r} \frac{c_m}{s - a_m} + d + se \tag{5}$$

Nr is the order of the reduced-order model (Nr<<N). This reduced-order model $\tilde{G}(s)$ can capture the input-output dynamic characteristics of the original flow field system in the frequency band of interest with high accuracy and at extremely low computational cost.

2.2 Numerical simulation methods and feedback control scheme

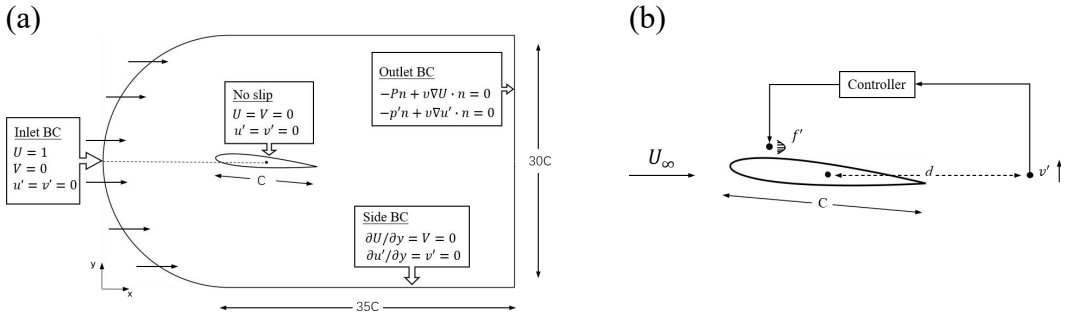

Fig. 1 (a) flow field computational domain and boundary conditions; (b) Schematic of the closed-loop feedback control system

To verify the effectiveness of the aforementioned control theory, this paper employs Direct Numerical Simulation (DNS) to construct a numerical simulation environment for the flow around a two-dimensional NACA0012 airfoil at a low Reynolds number. All computations are implemented within the open-source finite element platform FEniCS. Regarding the numerical solution, spatial discretization adopts the Taylor-Hood mixed finite element scheme to ensure numerical stability. Unsteady time advancement utilizes a second-order Backward Differentiation Formula (BDF2), with the time step set to $\Delta t = 5 \times 10^{-4}$. The decoupling of velocity and pressure is achieved through the Incremental Pressure Correction Scheme (IPCS).

The computational domain and boundary conditions are shown in Fig. 1(a). Type-C block mesh is locally refined on the airfoil surface and in the wake region. The height of the first layer of the mesh on the wall is y+= 0.01 and the total number of elements is approximately 9.6×10^5.

We arranged the actuator and sensor in the physical space as follows, as shown in Fig. 1(b), a body force f′ is applied on the upper surface of the airfoil near the leading edge as the input. Its spatial distribution is determined by the input matrix B and takes the form of a Gaussian distribution function S(x, y):

$$S(x,y) = \frac{1}{2\pi\sigma^2}\exp\left(-\frac{(x-x_c)^2+(y-y_c)^2}{2\sigma^2}\right) \tag{6}$$

where (x_c, y_c) represents the actuation center, and σ controls the range of action. This smooth body force can effectively simulate the momentum injection into the boundary layer by an actuator or synthetic jet.

A velocity probe is placed downstream of the airfoil at a distance d from the chord center to monitor the vertical velocity perturbation v′ in real-time. This measured value is processed by the control law and fed back to the input, forming a closed loop.

Based on the identified reduced-order model $\widetilde{G}$, this paper adopts the H_∞ loop-shaping method proposed by Glover & McFarlane to design a robust controller.

To meet the specific performance requirements for flow control, we have pre-defined the mathematical structure of the weighting functions and treated key parameters as variables to be optimized:

$$W_1(s) = k_1\frac{s+\omega_z}{s}\frac{\omega_i}{\omega_z}, \quad W_2(s) = \frac{\omega_h}{s+\omega_h}\frac{s^2/\omega_r^2 + 2\xi_z s/\omega_r + 1}{s^2/\omega_r^2 + 2\xi_p s/\omega_r + 1} \tag{7}$$

where W_1 is the pre-compensator weight, and W_2 is the post-compensator weight. The controller tuning is formulated as a nonlinear constrained optimization problem solved by MATLAB's fmincon, where the parameters $\theta = [k_1, \omega_i, \omega_z, \xi_p, \xi_z, \omega_h]^T$. are adjusted to achieve the optimal stability margin b_{opt}.

3. Result

3.1 Frequency and Time Domain Validation

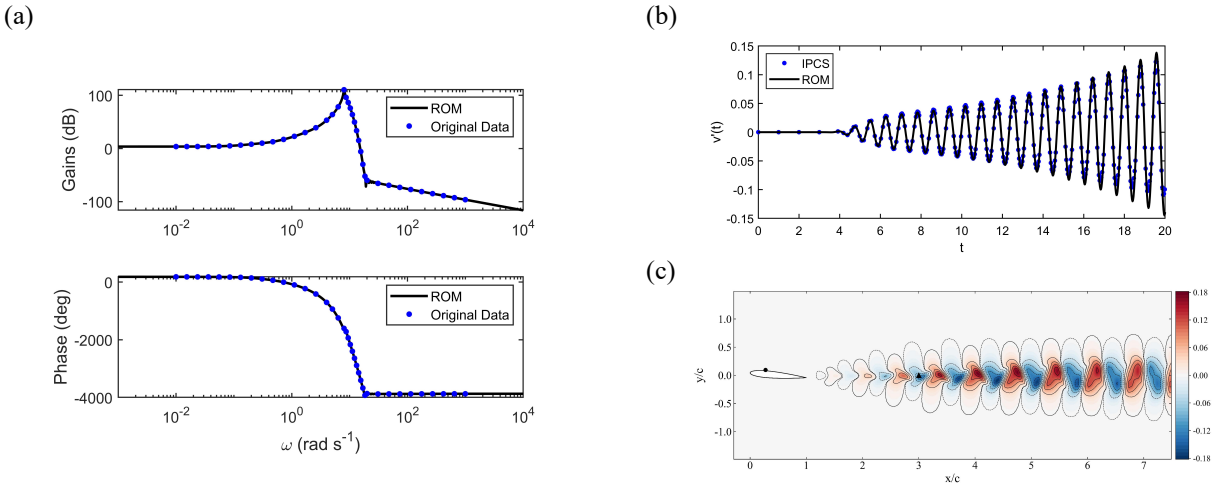

Fig. 3 validation of the reduced-order model (ROM). (a) Bode plot of the open-loop system; (b) Open-loop impulse response; (c) Contour plots of the linear frequency response at the domainant frequency

To verify the effectiveness of the reduced-order model, we selected an unstable operating conditions for analysis: For Case $(Re = 2300, \alpha = 5°)$ actuator is located at (x/c, y/c) = (0.275,

0.094). We perform a frequency scan of the high-dimensional linear system over a broadband range (10-2~103rad/s). As shown in Fig. 3(a), the Reduced-Order Model (ROM) identified using the VECTFIT algorithm coincides highly with the original data on the gain and phase curves of the Bode plot. The fitting RMS error is below 10-5, indicating that the ROM accurately captures the linear frequency-domain characteristics of the system.

Further validation using time-domain impulse response, as shown in Fig. 3(b) demonstrates that the output trajectory of the ROM matches well with the nonlinear DNS (IPCS) simulation results at the sensor location (x/c=3.0). During the linear growth phase (t < 15s), the two trajectories are nearly identical, accurately reflecting the instability characteristics where flow perturbations grow exponentially with time, as well as the dominant frequency. The minor deviation observed after t > 18s is attributed to the dominance of strong nonlinear effects in the actual flow field; however, within the linear range used for feedback control design, the model's accuracy is fully sufficient.

To deeply reveal the spatial evolution mechanism of flow instability, the transient flow field from time-domain Direct Numerical Simulation at t=20s is shown in Fig. 3(c). The flow field intuitively exhibits typical convective instability characteristics: minute perturbations generated by the actuator undergo significant spatial amplification while convecting downstream, forming a symmetric wavepacket structure that gradually diverges along the flow direction. The topological structure of this transient field, including the wavepacket shape, wavelength, and spatial growth trend, is consistent with the linear response mode predicted in the frequency domain. This confirms that the linear system can accurately capture the dominant instability modes in the flow field.

3.2 Closed-Loop Control Effectiveness

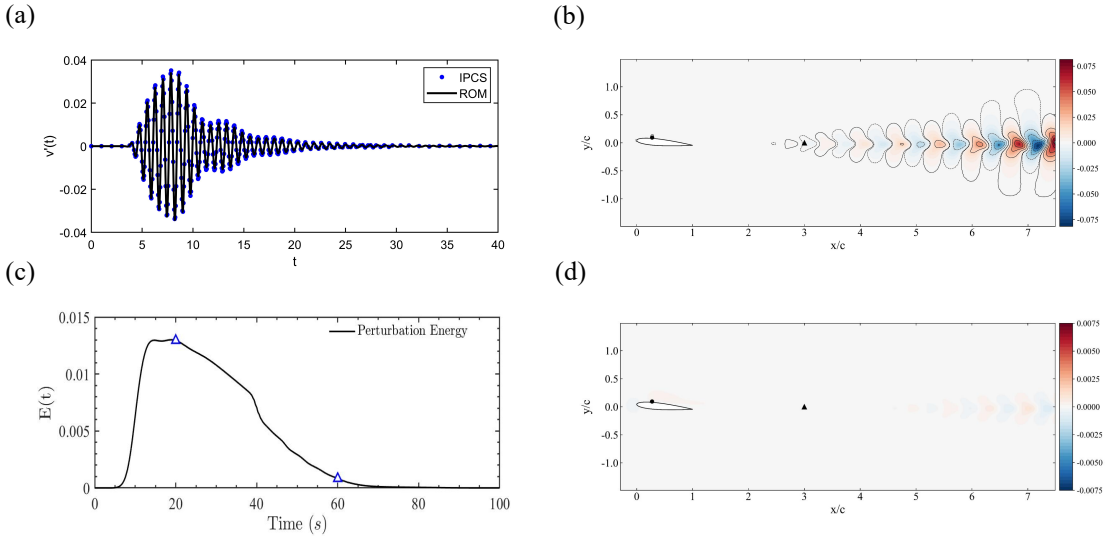

Fig. 4 Flow field evolution under closed-loop control. (a) Comparison of transverse velocity between and ROM; (c) Evolution of the total disturbance energy E(t); (b, d) Contour plots of transverse velocity under control at t=20s and t=60s

Applying the designed control laws to the direct numerical simulations. Fig. 4 demonstrates the evolution process of the closed-loop system in time and space.

From the velocity fluctuation-time curves at the sensor location, as shown in Fig. 4(a) it can be seen that in the initial stage, due to the convective instability of the flow field, the disturbances undergo a brief period of growth. However, with the intervention of the feedback control loop, the velocity fluctuations are rapidly suppressed and eventually converge to zero. Moreover, the predicted trajectory of the ROM maintains extremely high consistency with the actual DNS simulation results throughout the entire control process.

The evolution of the global perturbation energy E(t), as shown in Fig. 4(c) further quantifies the control effectiveness. Total field disturbance energy reached its peak at t ≈ 20s, and local

fluctuations at the sensor location at t=20s have been significantly weakened by the controller, far lower than those in the uncontrolled open-loop flow field, compared with shown in Fig. 3(d).

After the suppression effect of the controller persists for a certain period until t=60s, the global perturbation energy E(t) of the flow field is greatly reduced, and the large-scale vortex structures in the wake have been completely eliminated, as shown in Fig. 4(d). The flow field returns to a stable laminar base flow state, proving that the closed-loop system has achieved global stabilization of the flow field.

3.3 Optimization and Analysis of Sensor Placement

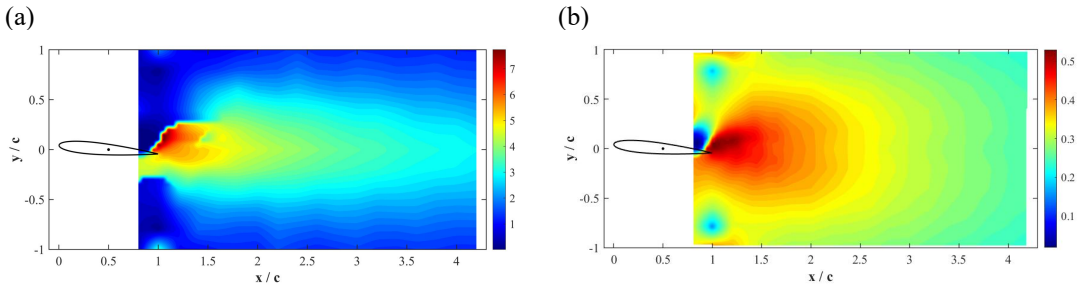

Fig. 5 The influence of sensor location on control performance. (a) Spatial distribution of the minimum Euclidean distance δ_{pz}; (b) Spatial distribution of the optimal stability margin b_{opt}

To further improve the control performance, we conducted spatial optimization of the sensor placement. For every spatial grid point in the wake region downstream of the airfoil, we treated it as a sensor location to re-identify the reduced-order model, and iteratively optimized the weight parameters to obtain the optimal stability margin at that location.

From Fig. 5(b), which shows the spatial distribution contour maps of b_{opt} for case, it can be seen that the stability margin exhibits significant non-uniformity in space, with distinct high-performance regions. This indicates that the choice of sensor location has a decisive impact on the robustness of the control system.

We introduce the minimum Euclidean distance index between poles and zeros, δ_{pz}, from control theory. For flow systems with unstable poles (RHP Poles), Right-Half Plane zeros (RHP Zeros) represent the non-minimum phase characteristic of the system, introducing additional phase lag, thereby severely limiting the bandwidth and performance of feedback control. δ_{pz} is defined as the minimum geometric distance between an RHP pole (p_i) and all RHP zeros (z_j) in the complex plane. This index quantitatively describes the degree to which the most dangerous zero approaches the unstable pole in the system.

Comparing the spatial distribution of the minimum Euclidean distance between poles and zeros δ_{pz} with the spatial distribution of the optimal stability margin b_{opt} obtained through actual optimization, a strong positive correlation is presented in their spatial patterns: in regions where δ_{pz} is large, the system is not limited by severe bandwidth constraints, and thus a higher stability margin b_{opt} can be achieved through parameter optimization; conversely, in regions where δ_{pz} is small, b_{opt} drops sharply due to the phase lag and lack of observability caused by the proximity of zeros and poles.

4. Summary

This paper addressed the problem of flow separation and unsteady vortex shedding over a NACA0012 airfoil at low Reynolds numbers. A resolvent-based modeling framework for the linearized Navier – Stokes equations was combined with an H_∞ loop-shaping strategy to construct a feedback control system, which was assessed using direct numerical simulations (DNS). The main research are as follows:

A low-dimensional reduced-order model (ROM) was identified from the system frequency response using the Vector Fitting technique. Frequency- and time-domain validations demonstrate that the ROM accurately reproduces the high-dimensional linear frequency response and transient input–output dynamics of the flow at very low computational cost.

Based on this ROM, an H_∞ robust controller was designed and implemented via a localized body force actuator on the suction side of the airfoil. In the tested case, the controller effectively suppresses laminar separation and large-scale vortex shedding in the wake, rapidly attenuates velocity fluctuations at the sensor location, and drives the global perturbation energy towards zero, thereby achieving global stabilization of the flow with satisfactory robustness.

A spatial traversal of candidate sensor locations, shows that the optimal stability margin b_{opt} exhibits a highly non-uniform spatial distribution, indicating that sensor placement has a decisive influence on closed-loop performance.

The spatial variation of b_{opt} is found to correlate strongly and positively with the minimum RHS pole–zero separation δ_{pz}. This reveals that the phase lag and loss of observability associated with RHP zeros approaching unstable poles are the fundamental physical mechanisms limiting the feedback control performance. Optimal sensor locations should be chosen in regions where δ_{pz} is large to avoid pole-zero cancellation and to maximise the achievable robustness margin.

Acknowledgment

This research is supported by the National Natural Science Foundation of China (Youth Program, Grant No. 12302363) and Aeronautical Science Fund (Grant No. 2024Z034052005].

References

[1] CHOI H, JEON W P, KIM J. Control of flow over a bluff body[J]. Annual Review of Fluid Mechanics, 2008, 40: 113-139.

[2] COLONIUS T, WILLIAMS D R. Control of vortex shedding on two- and three-dimensional aerofoils[J]. Phil. Trans. R. Soc. A, 2011, 369(1940): 1525-1539.

[3] MCKEON B J, SHARMA A S. A critical-layer framework for turbulent pipe flow[J]. Journal of Fluid Mechanics, 2010, 658: 336-382.

[4] TOWNE A, LOZANO-DURÁN A, YANG X. Resolvent-based estimation of space–time flow statistics[J]. Journal of Fluid Mechanics, 2020, 883: A17.

[5] SIPP D, MARQUET O. Characterization of noise amplifiers with global singular modes: the case of the leading-edge flat-plate boundary layer[J]. Theoretical and Computational Fluid Dynamics, 2013, 27(5): 617-635.

[6] SYMON S, SIPP D, MCKEON B J. A tale of two airfoils: resolvent-based modelling of an oscillator versus an amplifier from an experimental mean[J]. Journal of Fluid Mechanics, 2019, 881: 51-83.

[7] YEH C, TAIRA K. Resolvent-analysis-based design of airfoil separation control[J]. Journal of Fluid Mechanics, 2019, 867: 572-610.

[8] JIN B, ILLINGWORTH S J, SANDBERG R D. Feedback control of vortex shedding using a resolvent-based modelling approach[J]. Journal of Fluid Mechanics, 2020, 897: A26.

[9] GLOVER K, MCFARLANE D. Robust stabilization of normalized coprime factor plant descriptions with H_∞-bounded uncertainty[J]. IEEE Trans. Autom. Control, 1989, 34(8): 821-830.